

Dynamically Reconfigurable Sources for Arbitrary Gaussian States in Integrated Photonics Circuits

Aharon Brodutch,^{1,2,3,*} Ryan Marchildon,^{1,†} and Amr S. Helmy^{1,2,‡}

¹*The Edward S. Rogers Department of Electrical and Computer Engineering,
University of Toronto, 10 Kings College Road, Toronto, Ontario M5S 3G4, Canada.*

²*Center for Quantum Information and Quantum Control,
60 St George St., Toronto, Ontario, M5S 1A7, Canada*

³*Department of Physics, University of Toronto, 60 St George St., Toronto, Ontario, M5S 1A7, Canada*

We present a modular design for integrated programmable multimode sources of arbitrary Gaussian states of light. The technique is based on current technologies, in particular recent demonstrations of on-chip photon manipulation and the generation of highly squeezed vacuum states in semiconductors and generates a very broad range of Gaussian states. While the design is generic and is not dependent on any platform for realistic realization, we adopt recent experimental results on compound semiconductors as a demonstrative example. Such a device would be valuable as a source for many quantum protocols that range from imaging to communication and information processing.

Light provides an excellent platform for encoding quantum information that can be sent over long distances. In principle, the information encoded in light can be manipulated efficiently using currently available passive and active component, but many practical issues make the preparation and manipulation of such quantum states a difficult task in practice. While bulk optics provides a low-loss platform to manipulate information encoded in small photonic systems, scalability remains a major problem. Integrated optics offers an effective route to mitigate scalability challenges, and a number of demonstrations of state preparation and control in integrated optical devices have been reported recently [1–4]. These were designed with linear optics quantum computing in mind, assuming that the information is encoded in finite dimensional systems using single photons. In this work we show how to extend these schemes to the realm of continuous variable Gaussian states, by providing a blueprint for an integrated circuit that can be programmed and reconfigured to prepare any Gaussian state within a wide range of parameters. The design, approach and components utilized are based on currently available technologies, and rely on natural non-linearities in integrated waveguides to prepare initially squeezed vacuum states in multiple modes.

Most quantum information protocols have been designed for quantum systems with discrete degrees of freedom. These can be implemented using single photons with rail and/or polarization encoding [5]. However, such implementations suffer from several drawbacks. These include the need for synchronously generated single photons, photon-photon interactions that are difficult to achieve, gates that are probabilistic, and inefficient single-photon detection. Continuous variable (CV)

quantum information protocols that utilize light's continuous degrees of freedom offer several advantages over discrete approaches, in particular removing the requirement for single photons. In recent years both CV and hybrid CV/discrete approaches have been gaining significant momentum as alternative to their discrete counterparts for quantum information processing [6, 7].

In CV protocols, the initial states are usually Gaussian and can be generated from vacuum through a series of displacements, linear rotations, and squeezing [8]. Since these transformations are routinely achieved in bulk-optics, arbitrary Gaussian state generation seems straightforward in principle. In practice, however, the limited scalability and stability of bulk optics approaches is a hindrance to the development practical and large-scale quantum protocols, especially when the protocol must be scaled up to many modes, as required for example for CV cluster states [9, 10]. Moreover the requirement for in-line squeezing, i.e squeezing of an arbitrary state, which is simple in principle (usually by using $\chi^{(3)}$ non linearities), is difficult in practice even in bulk systems.

The ability to generate arbitrary multimode Gaussian states from an integrated chip would serve as an important milestone towards demonstrations of greater complexity and practical quantum technologies. Advances in the fabrication of integrated photonic circuits have made it possible to create large stable optical interferometers exhibiting low loss [11]. Moreover, semiconductor nonlinear waveguides have recently been used to produce highly squeezed vacuum states [12, 13]. Together, these components are sufficient for generating and manipulating Gaussian light.

In this work we describe a generic architecture for integrated photonic devices that can be programmed to prepare arbitrary N -mode Gaussian states. While it is known that such a device can be built in principle by using a sequence of rotations, squeezing and displacements, our design relies on a number of practical observations: 1-

*Electronic address: brodutch@physics.utoronto.ca

†Electronic address: ryan.marchildon@mail.utoronto.ca

‡Electronic address: a.helmy@utoronto.ca

It is much easier to generate squeezed vacuum states than to squeeze an arbitrary state. Consequently all squeezing is pushed to the beginning of the circuit. 2- It is possible to modify Paris's approximate displacement method [14] such that only a single displacement beam is needed, reducing the number of injected modes required from $\approx N$ to 3, regardless of N . 3- It is possible to control all elements using tunable phase shifters. As a result the device can be fully programmable using current technology. 4- The design is modular, allowing easy adaptation to different platforms and changing technologies. For example, it may be convenient to have each piece fabricated separately using a different platform. The resulting design allows a stable, programmable, scalable device that relies on current technological capabilities and can be easily adapted to different platforms.

I. MODULAR GENERATION OF ARBITRARY GAUSSIAN STATES

A state is called Gaussian if it has a Gaussian Wigner function; Equivalently an N mode state is a pure Gaussian state if and only if it can be generated from the vacuum by using a sequence of Gaussian operations [7, 15]. Those can be decomposed into a sequence of displacement $D([\alpha])$, rotation $R([\theta])$ and squeezing $S([\beta])$ operations, where the arguments are the multimode *displacement vector*, $[\alpha]$ *rotation matrix* $[\theta]$ and *squeezing matrix* $[\beta]$ (see Appendix A for details). While each of these operations can be implemented with a known optical component, a generic sequence is difficult to implement, with the biggest difficulty being the requirement for in-line squeezing, i.e squeezing of an arbitrary state. However, for Gaussian state generation it is possible to place the squeezing at the beginning of the sequence and generate single mode squeezed vacuum states in each mode (See Appendix A for the derivation) removing the requirement for in-line squeezing.

A realistic approach to state generation can be based on the decomposition

$$|G\rangle = D([\alpha])R([\zeta])S([\beta^{1m}])|0\rangle \quad (1)$$

where $[\beta^{1m}]$ is a diagonal squeezing matrix indicating only single mode squeezing. Furthermore, any N mode mixed Gaussian state can be created by tracing out N modes from a $2N$ mode purification which is also a Gaussian state. For this reason we can limit our discussion to pure Gaussian states without losing generality.

The decomposition of (1) implies the following stages for preparing an N mode Gaussian state:

1. Initialization of coherent beams with the same phase and relevant wavelengths in the relevant modes.
2. Preparation of N squeezed vacuum states (from coherent beams) in modes $1..N$, e.g using $\chi^{(2)}$ or $\chi^{(3)}$ non-linearities.

3. Rotation, consisting of an N -mode interferometer (on modes $1..N$).
4. Displacement, e.g by using the coherent beam to displace each mode ($1..N$) through a weakly-reflecting beam splitter or equivalent device.

A. Example: Generating pure a one-mode Gaussian state in bulk optics

To illustrate the ideas presented above, we briefly consider the generation of a pure one-mode arbitrary Gaussian state implemented using generic bulk optics components as shown in Fig. 1. The squeezing, rotation, and displacement transformations in phase space are depicted sequentially in Fig. 2. The scheme is as follows:

(i) Initialization: The protocol requires 2 phase locked beams, a signal wavelength λ_s (e.g. 1550 nm) for displacement and a pump wavelength λ_p (e.g. 775 nm) for generating the squeezed vacuum. In general it is useful to have an additional phase-locked beam of wavelength λ_s to use as a reference or local oscillator (LO) for subsequent homodyne detection. A common approach is to coherently split a high intensity beam at λ_s 3 ways, with one beam used to generate the λ_p pump via second harmonic generation (SHG) in a nonlinear crystal 'doubler' (e.g. BiBO). The squeezed light generated at wavelength λ_s by this pump (see below) maintains a stable relative phase with respect to the other two beams.

(ii) Squeezed vacuum preparation: Squeezing (see Fig. 2 ii) is most often obtained through nonlinear wave-mixing processes, such as spontaneous parametric down-conversion (SPDC) in a second-order nonlinear medium [16, 17]. This is done for example by using a periodically-poled lithium niobate (PPLN) waveguide designed for squeezed light generation in the telecom C-band at $\lambda_s = 1550$ nm with a pump field at $\lambda_p = 775$ nm. When operated in the single-pass configuration without optical feedback from a cavity, the output is a squeezed vacuum field at 1550 nm having squeezing parameter r with proportionality $r \propto \chi_{eff}^{(2)} |A_p| L$, where $\chi_{eff}^{(2)}$ is the effective non-linearity and L is the waveguide length [18]. The squeezing parameter r is related to the phase-space quadrature variances by $\langle \Delta \hat{X}^2 \rangle = e^{-2r}/2$ and $\langle \Delta \hat{P}^2 \rangle = e^{2r}/2$. Where the quadratures are defined as $\hat{x} = (\hat{a} + \hat{a}^\dagger)/\sqrt{2}$ and $\hat{p} = (\hat{a} - \hat{a}^\dagger)/i\sqrt{2}$. The upper bound on r is set by the parametric gain of the nonlinear medium, determined by both practical and physical limitations on A_p , L , and $\chi_{eff}^{(2)}$. The largest r measured in a squeezed state to date is $r = 1.73$ [19], equivalent to 15 dB below the classical shot noise level.

(iii) Rotation: Arbitrary rotations in the single-mode (see Fig. 2 iii) case are straightforward, requiring only a single phase-shifter to modify the relative phase with the reference or LO. Note that by convention, all rotations due to phase shifts, reflections and free evolution are defined in a clockwise (CW) sense relative to the quadrature

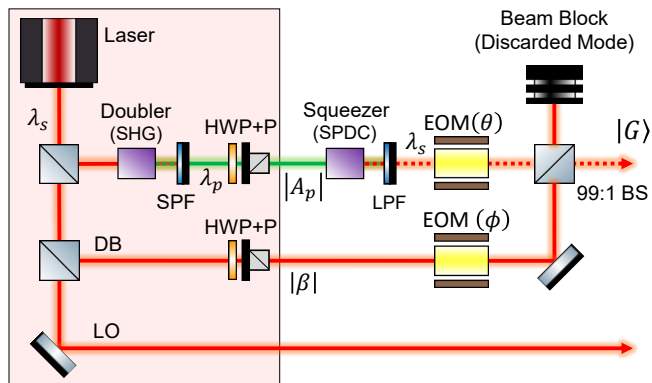


FIG. 1: One-mode Gaussian state generation with bulk optics. The initialization stage, highlighted in red, is also used in the N -mode protocol. Squeezed vacuum is generated through SPDC followed by a low pass filter (LPF) to remove the pump. An electro-optic modulator (EOM) is used to generate a phase shift. Displacement is generated via mixing with a high power phase-locked coherent state. Acronyms: HPF = high pass filter; DB = displacement beam; LO = local oscillator; HWP+P = half wave plate and polarizer for amplitude control.

axes, as shown in Fig. 2.

(iv) Displacement: The displacement operator $D(\alpha)$ (see Fig. 2 iv) can be approximated by mixing the squeezed state with a bright coherent state $|\alpha_0\rangle$ at a beamsplitter (or equivalent mode coupling device) [14] with reflection coefficient $\eta \ll 1$ such that $\sqrt{\eta}\alpha_0 = \alpha$. The limitations of this method are discussed in Sec B and the fidelity between the desired state and the actual state is plotted in fig 3 for different states and values of η .

II. GENERATION OF ARBITRARY N -MODE GAUSSIAN STATES ON-CHIP

The construction implied by (1) can be used as a basis for a tunable on-chip N mode Gaussian state generator. Below we describe a generic approach for building such a device, using four key modules. We then move to the simplest non-trivial example, a tunable two mode pure Gaussian state generator, using AlGaAs as a model platform. Tunability in the AlGaAs example (see Fig 4) is achieved using variable phase shifters. This allows a single approach in the generic case, although it is possible to combine it with tunable directional couplers.

A. Generic modular approach

Recent work demonstrating on-chip squeezing [12, 20, 21], tunable phase-shifts [22, 23], and arbitrary linear optical transformations [11] have assembled all the key ingredients necessary for independent control of $S([\beta^{1m}])$, $R([\theta])$, and $D([\alpha])$ in an integrated quantum circuit. In

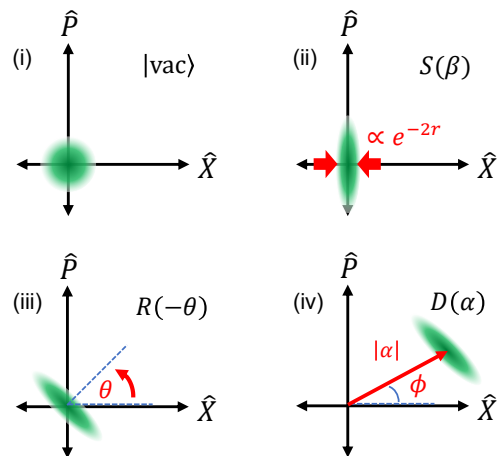


FIG. 2: Phase-space depiction of the four stage process. A one-mode vacuum state (i) is squeezed (ii), rotated (iii) and displaced (iv).

the generic setting we consider each of the four stages as an independent module that can be fitted to the desired platform. Our aim is to show that the technology for each module has already been demonstrated and to suggest possible implementations.

Initialization: The initialization stage consists of preparing coherent 775 nm beam (pump) for use as a source for SPDC and 1550 nm for both the displacement and as a reference, all beams must be phase coherent. In principle a nonlinear waveguide that is phase-matched for SPDC with 775 nm can also achieve the 1550 nm-to-775 nm SHG, in practice this is limited by the amount of optical power that can be handled by the chip without burning facets or inducing unwanted nonlinearities. However, in many quantum information processing tasks coherence with an external reference should be maintained. We therefore consider the same external pumping as in the single-mode case of Sec. IA (see initialization stage in fig 1). The use of this external initialization stage does not affect scalability since the architecture suggested requires only two beams (the 1550 nm displacement beam and the 775 nm beam) to be injected into the device, regardless of N .

Generation of squeezed vacuum: The key requirements for an on-chip source of strong squeezing are a high effective nonlinearity, low optical loss, and a long interaction length that is typically facilitated by the use of cavities due to limitations on the pump power. An on-chip squeezed light source based on low-loss silicon nitride microrings was recently demonstrated [12], where by controlling integrated microheaters to modify the cavity coupling, the measured squeezing was electrically tunable between 0.5 dB and 2 dB (corresponding to 0.9 dB and 3.9 dB when corrected for losses). This approach utilized a four-wave-mixing process stemming from third-order ($\chi^{(3)}$) nonlinearities. In another approach, which utilized parametric downconversion from second-order

($\chi^{(2)}$) nonlinearities in a periodically-poled lithium niobate waveguide resonator [21], 2.9 dB of squeezing (corresponding to 4.9 dB in the lossless case) was directly measured. Both of these examples used continuous-wave pumping. Utilizing the higher peak powers and hence larger effective nonlinearities available through femtosecond pulsing can offer even higher degrees of squeezing. In Sec. II B, we describe an architecture based on AlGaAs that may be capable of producing squeezing in excess of 10 dB in a single-pass configuration under fs-pumping, before losses and detector efficiencies are taken into account. Programmable Mach Zehnder interferometers (see Fig. 4 and Sec. II B) can be used to tune the squeezing parameter by attenuating the pump. Once squeezed light has been generated, the pump is typically filtered to prevent it from causing unwanted nonlinear phase modulation or squeezing elsewhere in the circuit. Common methods of filtering are wavelength demultiplexers built from asymmetric coupled waveguides [24], ring resonator filters, or Bragg reflector gratings [25] which utilize the photonic bandgap effect.

Rotation: A generic rotation $R([\alpha])$ can be generated efficiently using an array of linear optics elements (beam splitters and phase shifters) [26, 27]. In integrated circuits, tunable low-loss phase shifters can be achieved thermo-optically using resistive heaters to modify the local refractive index [22], or electro-optically using bias voltages [23], where the optimum choice depends on the material system. For example, AlGaAs circuits benefit from a strong electro-optic Pockels effect owing to a large intrinsic $\chi^{(2)}$ nonlinearity [23], whereas silicon-on-insulator (SOI) circuits possess a relatively strong thermo-optic effect [11]. Beam-splitting transformations can be provided by directional couplers which evanescently couple optical modes between adjacent waveguides [28], or multi-mode interferometers (MMIs) which work based on self-imaging effects [29]. 3D multiport splitters can also be realized on-chip [30], but planar nearest-neighbour coupling remains the most compatible with conventional fabrication techniques. In-situ tunability over the splitting ratio is commonly achieved by concatenating a pair of two-mode splitters with a tunable phase shifter in one path between them, forming a MZI [23]. An MZI with a tunable internal phase ϕ to control its splitting ratio, followed by an additional external phase shift θ in one outgoing arm, becomes the basic unit cell of reprogrammable circuits for universal rotations (see Fig. 4). Recently, Harris et al. demonstrated a reprogrammable SOI quantum photonic chip comprised of 56 MZIs and 213 phase shifters [11].

Displacement: It is possible to use Paris's method [14] for approximating the displacement operator $D([\alpha])$ by pairing each mode with an ancillary strong coherent state mode and displacing each mode individually. However, such an architecture would be cumbersome to engineer with 2D planar waveguides and makes inefficient use of chip real-estate. Instead it is possible to use a single ancilla mode (mode 0) containing a strong coherent

state $|\alpha_0\rangle$ that cascades through an array of strongly cross-coupling mode splitters, displacing each mode sequentially as depicted in Fig. 3(a). In our notation this can be written as a rotation $R([\Delta]) = \prod_k T_k$ where T_k is a two-mode splitter transformation between modes k and $k - 1$ with reflection coefficient η_k .

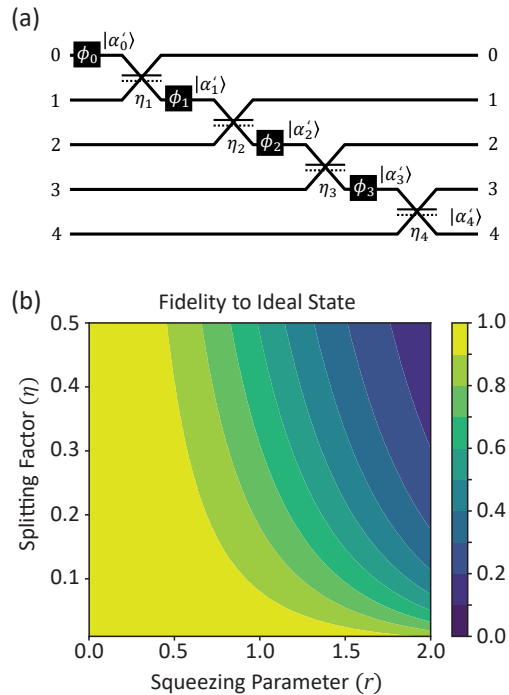


FIG. 3: (a) The cascaded displacement scheme for $N = 4$. At each step, a strong coherent state $|\alpha'_k\rangle$, in mode k is used to displace mode $k + 1$ by $\alpha_{k+1} = \alpha'_k \sqrt{\eta_k}$ and swap with that mode using a beam splitter with reflectivity $\eta_k \ll 1$. Note that the final modes are shifted by -1 with respect to the original modes so that the final mode N is the ancilla which is discarded. (b) Fidelity between a squeezed state after an approximate displacement and the corresponding displaced squeezed state (see Sec. III A). For a fixed value of α_0 , the fidelity depends on the reflection coefficient factor η and the squeezing parameter r for mode 1, which in turn relates to the average number of photons. More photons and higher η will increase the probability of photons ‘leaking’ to the ancilla mode.

At each coupling intersection, the strong coherent beam in mode $k - 1$ displaces the state in mode k and then the modes swap. In order to achieve this the reflection coefficient η_k must be small, $\eta_k \ll 1$ (i.e most of the light from mode k is transmitted to $k - 1$ and vice versa). If $|\Psi\rangle = R([\zeta])S([\beta^{1/m}])|0\rangle$ is the state before the displacement, the approximate transformation can be written as (see Appendix B for details):

$$\begin{aligned}
 & R([\Delta])D_0(\alpha_0)|\Psi\rangle \otimes |\text{vac}\rangle_0 \\
 & \approx D_N(\alpha_N)P_{\uparrow} \prod_{k=0}^{N-1} D_k(\alpha_k)|\Psi\rangle \otimes |\text{vac}\rangle_0 \quad (2)
 \end{aligned}$$

where ; P_{\uparrow} is a permutation of modes that takes $0 \rightarrow N$ and $k \rightarrow k - 1$ for all $k \in \{1, \dots, N\}$; In Fig 3 the operator P_{\uparrow} represents the fact that the state to be displaced has input modes 1, 2, 3, 4 and corresponding output modes 0, 1, 2, 3.

The displacement of each individual mode can be controlled by tuning the splitting factor η_k of each mode coupler and rotating the phase, while taking into account all η_m and α_m for which $m < k$. Tunability in η_k can be achieved by implementing the mode coupler as an MZI with phase control [11, 23], or through by electro-optically or thermally inducing a modal mismatch between the two coupled waveguides [31]. Adding phase shifters ϕ_k between stages to tune the phase of each $|\alpha_k\rangle$ allows control over the displacement angle.

The first correction for the approximate displacement comes from the possibility that some photons from the displaced mode will leak into the displacement beam (see Methods sec. B). Experimentally it is possible to put bounds on this error by blocking the displacement beam and counting the number of photons exiting port N . In general, the approximation will not be a dominant source of error as long as η_k is small compared to the probability that a single mode will lose a photon elsewhere in the circuit. In sec. III A (see also Fig. 2 b) we give a numerical example of the bounds on this approximation in the single mode case.

B. Example: Arbitrary two-mode Gaussian states generated in an AlGaAs integrated circuit

The simplest scenario illustrating all elements of the architecture described above is a device for generating arbitrary pure two-mode Gaussian states as shown in the circuit in Fig. 4 (a). We use AlGaAs as an example platform since it offers a broad range of quantum-circuit functionalities, including electro-optic tuning, self-pumped electrically-injected quantum state generation, and on-chip single photon detection [23, 33–35] (the latter two are not directly useful for our design, but could become useful in various extensions, for example generation of non-Gaussian states). It also supports a large intrinsic second-order ($\chi^{(2)}$) optical nonlinearity that facilitates the generation of highly-squeezed states. In particular, recent results indicate squeezing parameters of $r > 3$ in AlGaAs waveguides [36]. Here we consider the degenerate Type I parametric process where the downconverted photons are identical in frequency, polarization, and spatial mode. This allows a coherently-pumped array of parallel one-mode squeezers.

The circuit layout is shown in Fig. 4(a), where eleven electrodes provide dynamic reconfigurability through electro-optic phase shifts, and MZIs serve as variable beamsplitters. To split the injected pump equally between the two parametric generator paths, we use a 1-by-2 port MMI due to the robustness of its fixed 50:50 splitting ratio against fabrication imperfections which elimi-

nates the need for additional electrodes. Electrodes v1 and v3 adjust the fraction of pump power injected into the parametric generators, thereby tuning the squeezing, with v2 and v4 providing phase control. A Bragg reflection grating (BRG) filter blocking the ‘signal’ wavelength of 1550 nm is used to define the start of the parametric generator, while a second BRG blocking the 775 nm pump terminates it. The parametric generator is a segment of the nonlinear waveguide that is narrowed in width. The narrowing adjusts the modal dispersion of the waveguide such that phase-matching is satisfied for 775 nm only within the narrowed segment, with the phase-matching tuning curve (e.g. see Fig. 2 in Ref. [37]) shifting to shorter pump wavelengths as the waveguide width is increased [38]. Together with the BRGs, this provides a strategy for restricting squeezed light generation to only the desired region while preventing it elsewhere within the nonlinear circuit. Following squeezed light generation, arbitrary $U(2)$ rotations are provided via electrodes v5-v7, with v5 controlling the two-mode-mixing between modes 1 and 2. Finally, displacements are controlled by electrodes v8-v11 (as in Fig. 3(a)), where the MZIs are operated near conditions of perfect cross-coupling (mode swapping) with $\eta \approx 0$, and the displacement beam cascades sequentially through each mode before being discarded.

State evolution through the circuit was simulated using the symplectic transformation method [7, 39]. Fig. 4(b) depicts the electrode voltages and corresponding output states for five different configurations. For readability we have re-normalized the voltage values to the following mappings: for squeezing $v1, v3 \in [0, 1] \rightarrow r \in [0, r_{\max}]$, where in this case we show tuning up to $r_{\max} = 1$ (8.7 dB); for single-mode phase rotations $v2, v4, v6, v7 \in [0, 1] \rightarrow \theta \in [0, \pi]$; for two-mode mixing $v5 \in [0, 1] \rightarrow \eta \in [1, 0]$; for displacement angle $v8, v10 \in [-1, 1] \rightarrow \phi \in [-\pi, \pi]$; and for displacement magnitude $v9, v11 \in [0, 1] \rightarrow \eta \in [0, 0.0125]$, where the resultant displacement of mode k is $D_k(\alpha_k \sqrt{\eta_{k+1}})$ (see Fig. 3(a)) and we have set $|\alpha_0| = 40$ as the magnitude of the injected displacement beam after coupling into the circuit. Note that we remain under the estimated bound of $\eta \leq 0.0180$ needed to maintain fidelities of 98% or greater with the ideal displaced state (see Sec. B).

Fig. 4(c) shows two Wigner function slices from the output state, computed for each configuration after tracing out the discarded ancilla mode. The (x2, p2) slice shows the quadrature evolution in mode 2, while the (x1, x2) slice shows correlations between modes. In configuration (1) we begin with squeezed vacuum in mode 1 ($r = 0.75$ or 6.5 dB) and unsqueezed vacuum in mode 2. In configuration (2) we squeeze both modes equally ($r = 1$), rotating mode 1 by $\pi/4$ rad and displacing it by $|D| = [\langle \hat{x} \rangle^2 + \langle \hat{p} \rangle^2]^{-1/2} = 2.7$ photons (at an angle of $-\pi/4$ rad) to achieve an amplitude-squeezed state, and rotating mode 2 by $3\pi/4$ rad and displacing it by $D = 5.5$ photons (at an angle of $-\pi/4$ rad) to achieve a phase-squeezed state. In (3) we mix two single-mode

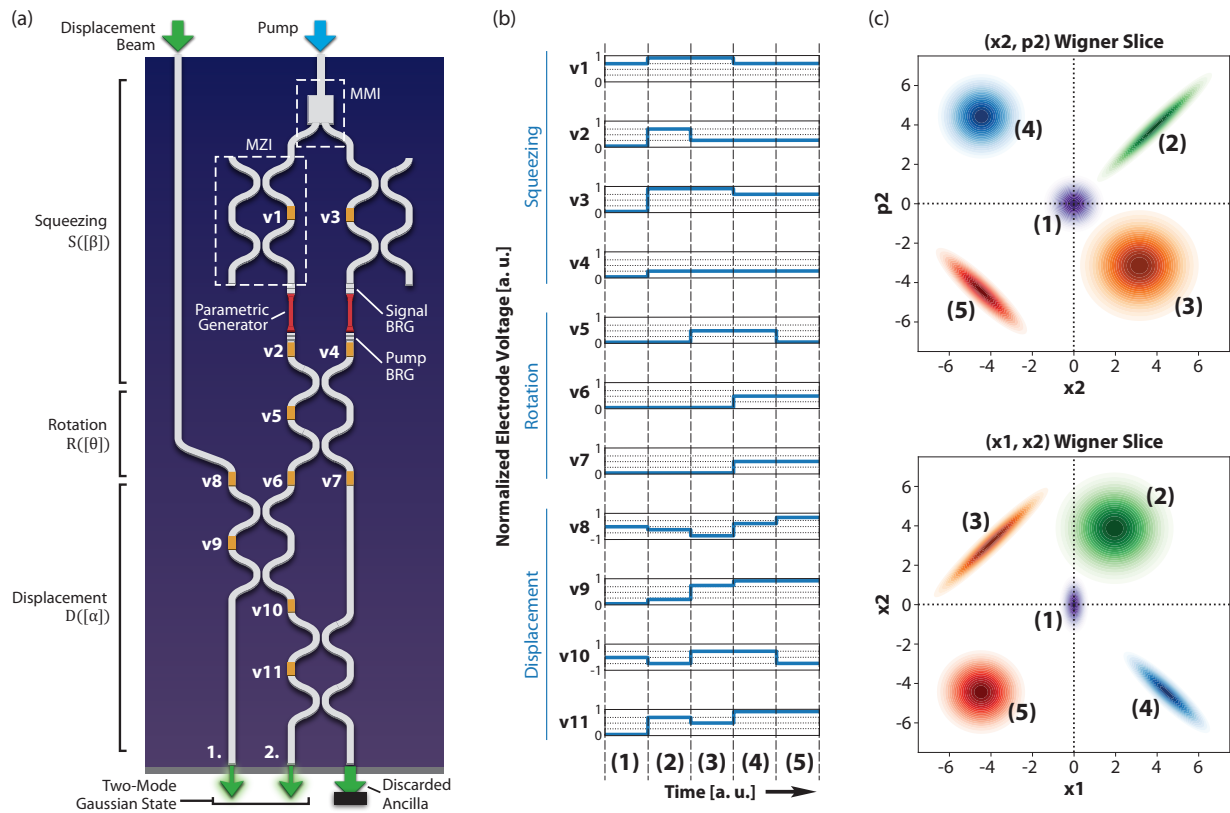


FIG. 4: (a) Schematic of dynamically reconfigurable AlGaAs circuit for generating arbitrary two-mode pure Gaussian states. The device includes the three reconfigurable modules (squeezing, rotation and displacement). The initialization module is external and assumed to be the same as in Fig. 1. The 11 electrodes can be used to program the state II B). Five example settings (b) generate the five states depicted in (c).

squeezed states at a 50:50 splitter to achieve a two-mode squeezed state as seen by the correlations in the (x_1, x_2) Wigner slice. In (4) we use phase-shifts at v_6 and v_7 to rotate the (x_1, x_2) correlations, while further increasing the displacement of both modes via v_9 and v_{11} . In configuration (5) we revert back to two single-mode squeezed states, but in a different quadrant of phase space.

The phase shifters envisaged in Fig. 4 are based on electro-optic modulation as seen in previous AlGaAs quantum circuits [23]. Circuit reconfigurability can be achieved using a myriad of techniques, some being more favourable than others depending on the specific needs of the application. Electro-optic and thermal tuners have the advantage of being implementable monolithically on the same platform as passive components, with the former capable of achieving modulation speeds in the GHz, while the latter is limited by the thermal time constant but can achieve switching speeds in the MHz when appropriately designed. In cases where performance enhancements such as higher speed, better switching extinction, or lower bias voltages are needed, advanced coupler designs such as grating-assisted, asymmetric, or ring-resonator couplers can be used at the expense of a reduced operating bandwidth [40–42]. Whereas a simple electro-optic MZI coupler may need tens of volts to a few

volts of bias, a ring resonator coupler can require merely a fraction of a volt. In some cases, flip-chip bonding with active devices may be appropriate, but this comes at the cost of increased optical loss, and hence is only really suitable for modulation of the pump. For example, rapid tuning of the squeezing parameter r can be achieved with speeds exceeding 10 GHz via absorption-based modulation of the pump using the quantum-confined stark effect [43] with flip-chip bonded III-V semiconductors.

III. CHALLENGES AND LIMITATIONS

The architecture provided is based on existing technologies. However, throughout this work we assumed that everything is ideal and neglected the corrections due to the approximate displacement stage. The approximation depends on how small we can keep η_k which in turn depends on the maximal displacement we want to allow. Consequently, there is a trade-off between the maximal displacement and the validity of the approximation. Below we give an explicit calculation of how well the displacement approximation works in the one-mode case and follow with a discussion of additional challenges

that will need to be addressed in a real device such as loss, and mode distinguishability.

A. Bounds for Single Displacement Stage

In real integrated circuits there are practical trade-offs between how small η is and our ability to precisely control it. Variability in η due to the stochastic nature of fabrication will be more pronounced when the target quiescent η is small. Accurate adjustment of $D_k(\alpha)$ through in-situ tuning of η may also be challenging if we are limited to $\eta \ll 1$. It is therefore useful to establish what upper bound on η still provides good fidelity to an ideal displacement transformation. We first consider the simple case of a single-mode squeezed vacuum state $|\psi\rangle$ displaced by an ancilla coherent state $|\alpha_0\rangle$, resembling the first stage in a multi-stage cascade. The total state before displacement is given by:

$$|\Psi\rangle = |\alpha_0\rangle_0 \otimes |\psi\rangle_1. \quad (3)$$

In the ideal case of a perfect displacement transformation, where we treat the approximation of Equation (2) as an equality, the output state is

$$|\Psi'\rangle_{\text{Ideal}} = D_0(\alpha_0\sqrt{\eta_1})R_0(\pi/2)|\psi\rangle_0 \otimes R_1(\pi/2)|\alpha_0\sqrt{1-\eta_1}\rangle_1,$$

whereas applying the standard mode-mixing transformation to the state gives the true output:

$$|\Psi'\rangle_{\text{Actual}} = U_{0,1}(\eta_1)[|\alpha_0\rangle_0 \otimes |\psi\rangle_1] \quad (4)$$

Fig. 3(b) shows the Uhlmann fidelity [32] of these two states $|\Psi'\rangle_{\text{Ideal}}$ and $|\Psi'\rangle_{\text{Actual}}$ computed as a function of η and squeezing parameter r . Under our assumptions of a pure squeezed vacuum state $|\psi\rangle$, we see that in the limit of $r \rightarrow 0$ (i.e. unsqueezed vacuum) the fidelity becomes 100% and is independent of η , which is the expected behaviour since we know $U_{0,1}(\eta_1)[|\alpha_0\rangle_0 \otimes |\text{vac}\rangle_1] = |\alpha_0\sqrt{\eta_1}\rangle_0 \otimes |-i\alpha_0\sqrt{1-\eta_1}\rangle_1$ which agrees with $|\Psi'\rangle_{\text{Ideal}}$ for all η . As the squeezing parameter r increases, we see that smaller η is required to ensure a high-fidelity transformation. To good approximation, the bound for obtaining a fidelity of at least F is given by $\eta \leq ar^{-b}$, where for $F \geq 95\%$ we have $\{a = 0.04265, b = 2.163\}$, and for $F \geq 98\%$ we have $\{a = 0.0181, b = 2.067\}$. As seen in Fig. 3(b), for squeezing of up to nearly $r = 0.5$ (4.3 dB), η can be kept relatively large at above $\eta = 0.1$ while still satisfying the approximation. However, for an input state with 15 dB of squeezing ($r = 1.73$) we require $\eta \leq 0.013$ and $\eta \leq 0.0058$ for fidelities of $F \geq 95\%$ and $F \geq 98\%$ respectively.

B. Squeezing

Squeezing in the waveguide can be increased by either increasing the length of the squeezing stage, or by increasing the 775 nm beam power. In practice too much

pump power can damage the device, have unwanted effects such as self phase modulation, or be self-limiting through two-photon absorption which increases with the pump intensity. Increasing length has two problems, first it will require a larger device, but more significantly it will increase loss (see below). As a consequence practical limitations will constrain the maximal squeezing per mode.

C. Loss

Minimizing optical loss is crucial to fully benefit from the squeezing achievable in a given platform. This can prove quite challenging in practice owing to how quickly the squeezing decays as loss increases. The amount of measurable squeezing falls as $S_T = 10 \cdot \log_{10} [T \cdot 10^{-S_0/10} + (1-T)]$ where S_0 and S_T refer to the measurable squeezing in dB before and after losses respectively, and T is the total transmission efficiency [18]. Hence, the 30 dB of squeezing achievable under lossless conditions by the AlGaAs platform described in Section II B, which surpasses the threshold of ~ 20.5 dB needed for fault-tolerant cluster-based quantum computing using Gottesman-Kitaev-Preskill (GKP) encoding [44], quickly falls below 20.5 dB for only 0.034 dB of optical loss. Optical losses in an integrated circuit can be caused by waveguide sidewall roughness, mode leakage at waveguide bends, reflections at material interfaces (such as the waveguide facets), or modal mismatches when coupling into and particularly out of the devices. Loss therefore poses the most problematic constraint for scalability, since for arbitrary rotations the device length grows quickly with the number of modes (around n^2 per the Reck scheme [26]), and loss is exponential in the circuit length. One possible mitigation strategy is entanglement distillation, which uses local non-Gaussian elements (such as photon counting) and sacrificial ancilla states to enhance the purity and correlations of a state subjected to loss [6, 45]. This can benefit from the relative ease in which a large number of ancillas can be prepared on an integrated chip compared to bulk approaches. Another distillation approach is to use heralded noiseless linear amplifiers [46, 47], which can be realized compactly in integrated optics, and in the case of AlGaAs, can even be monolithically embedded within the same platform [36].

IV. CONCLUSIONS AND OUTLOOK

We provided a generic architecture for a device that can prepare arbitrary multimode Gaussian states. The design is based on current technologies, for example AlGaAs integrated waveguides, and is kept modular so that it can be easily adopted for a variety of integrated platforms. It is fully programmable and can generate any Gaussian state up to some limitations that depend on

the specifics of the materials and the fabrication process (See Sec. III).

Gaussian states are a useful initial state for many quantum information protocols [7] including sensing [48] quantum communication [49, 50] and quantum computing [9]. A device that can generate arbitrary multi-mode Gaussian states be useful for generating the optimal states for these protocols, and will provide motivation for further research on optimization of CV protocols under realistic constraints such as loss. One further advantage of a programmable device (apart from versatility) is the ability to use feedback optimization methods such as those used recently in NMR to correct unknown imperfections [51, 52], fast reconfigurability would also allow to correct for optical phase drifts. Moreover, such a device opens the way for generating more general CV states, by placing detectors at some of the outputs and post-selecting a desired non-Gaussian state or even using adaptive schemes. In principle, the scheme can be modified to a device capable of performing arbitrary multi-mode Gaussian unitary operations, however such a device will require in-line squeezing which is very demanding in practice. Fast reconfigurability and appropriately placed time delays on some modes can also allow us to use time to encode larger states [53, 54].

Since the technology for implementing such a device is readily available, we expect to see a practical demonstration of our scheme in the near future. Such a demonstration would be a significant milestone for CV quantum information processing.

Acknowledgments

We thank Daniel James, Gleb Egorov and Armanpreet Pannu for discussions that lead to this work. This work was partially funded by the Center For Quantum Computation and Quantum Control, University of Toronto.

Appendix A: Gaussian states and unitaries

An N mode Gaussian unitary operation can be decomposed into an N mode rotation followed by N mode squeezing followed by N mode displacement [55]

$$U_G([\theta], [\beta], [\alpha]) = D([\alpha])S([\beta])R([\theta]); \quad (\text{A1})$$

Here $[\alpha]$, $[a^\dagger]$ denotes vectors with entries a_k , a_k^\dagger respectively; The displacement vector $[\alpha]$ has N complex entries α_k representing the displacement of each mode; The rotation matrix $[\theta]$ is an $N \times N$ unitary matrix with entries $\theta_{k,l}$; and the squeezing matrix $[\beta]$ is a complex, symmetric $N \times N$ matrix with entries $\beta_{k,l}$. These operators can be written in Fock notation as

$$\begin{aligned} \text{Displacement} & D([\alpha]) = e^{[\alpha]^\dagger [a^\dagger] - [\alpha] [a]} \\ \text{Rotation} & R([\theta]) = e^{i[a^\dagger]^T [\theta] [a]} \\ \text{Squeezing} & S([\beta]) = e^{[a^\dagger]^T [\beta] [a^\dagger] - [a]^\dagger [\beta] [a]}. \end{aligned}$$

A pure Gaussian state $|G\rangle$ is generated by $U_G([\theta], [\beta], [\alpha])|0\rangle$, however since a rotation at most adds a global phase to the vacuum state it is possible to remove the first rotation step:

$$|G\rangle = U_G([\theta] = 0, [\beta], [\alpha])|0\rangle. \quad (\text{A2})$$

(A1) and (A2) imply a generic procedure for producing any desired (pure) Gaussian state using a sequence of Gaussian operations). Our goal is to show that this can be done with only single mode squeezing initially as in (1).

To bring the squeezing matrix into diagonal form $S([\beta^{1m}])$ (i.e a form that implies only one mode squeezing) we use the following facts (see [8, 55]):

- $R([\zeta])S([\beta]) = S([\beta'])R([\zeta])$ such that $[\beta'] = e^{i[\zeta][\beta]}e^{i[\zeta]^T}$, where T means transpose.
- It is possible to bring any symmetric matrix $[\beta]$ into diagonal form using the Takagi factorization, i.e for any $[\beta]$ there exists a unitary U such that $[\beta^{1m}] = U[\beta]U^T$ is a diagonal matrix with non-negative entries.

From these facts it follows that we can write $U_G([\theta], [\beta], [\alpha]) = D([\alpha])S([\beta])R([\theta])$ to

$$U_G([\theta], [\beta], [\alpha]) = D([\alpha])R([\zeta])S([\beta^{1m}])R([\zeta])R([\theta]) \quad (\text{A3})$$

(see [56] for a more detailed derivation).

The above can be simplified further in the case of Gaussian states since $R([\zeta])R([\theta])|0\rangle$ is up to a global phase the same as $|0\rangle$, which leads us to (1).

Appendix B: Approximate displacement

The scheme in fig 3 generates an approximate displacement $D([\alpha])$ as well as a permutation of the modes when η_k is small enough. It is easier to see how well the approximation, (2) works by writing T_k in exponential form:

$$T_k = P_{k-1,k} e^{i\delta_{k-1,k}(a_{k-1}^\dagger a_k + a_k^\dagger a_{k-1})} e^{i(\phi_k - \phi_{k-1})a_{k-1}^\dagger a_{k-1}}$$

with $P_{k-1,k}$ being the operator that swaps modes $k-1$ and k , ϕ_k is the phase of α_k and $\sqrt{\eta_k} = \sin(\delta_{k-1,k}) = \frac{\alpha_k}{\alpha_0 \prod_{m=1}^{k-1} \cos(\delta_{m-1,m})}$, $\delta_{-1,1} = 0$. Note that for simplicity of the derivation we neglect any phases added by the cross-coupling since these can always be corrected.

Using the rules for switching the order of rotations and displacements, we can rewrite the transformation

$$\begin{aligned} & T_1 D_0(\alpha_0) \\ &= P_1 D_0(e^{-\phi_1} \alpha_0 \cos \delta) D_1(\alpha_1) e^{i\delta_{0,1}(a_0^\dagger a_1 + a_1^\dagger a_0)} e^{-\phi_1 a_0^\dagger a_0} \\ &= D_0(\alpha_1) D_1(e^{-\phi_1} \alpha_0 \cos \delta) P_1 e^{i\delta_{0,1}(a_0^\dagger a_1 + a_1^\dagger a_0)} e^{-\phi_1 a_0^\dagger a_0} \end{aligned}$$

which can be done for all terms, so that

$$\begin{aligned} \prod_{k=1}^N T_k D_0(\alpha_0) &= D_{0\dots N}([\alpha]) \times \\ & D_N \left[e^{i\phi_N} \alpha_0 \prod_{k=N}^N \text{Cos}(\delta_{k-1,k}) \right] \prod_{k=1}^N T_k \end{aligned} \quad (\text{B1})$$

where we use the ordering convention $\prod_{k=1}^N X_k = X_N X_{N-1} \dots X_1$. It is possible to ‘push’ the permutations to the left and get

$$\prod_{k=1}^N T_k = P_\uparrow \prod_{k=1}^N e^{i\delta_{k-1,k}(a_0^\dagger a_k + a_k^\dagger a_0)} e^{i(\phi_N) a_0^\dagger a_0} \quad (\text{B2})$$

Now taking $|\alpha_0| \gg 1$ such that $\delta_{k-1,k} \ll 1$ for all k we can see that $\prod_{k=1}^N T_k R([\theta]) S([\beta^{1m}]) |0\rangle \approx R([\theta]) S([\beta^{1m}]) |0\rangle$. With first order corrections being $\sum_k \delta_{k-1,k}(a_N^\dagger a_{k-1}) R([\theta]) S([\beta^{1m}]) |0\rangle$. These can be treated as possible photon losses.

-
- [1] M. Gräfe, R. Heilmann, M. Lebugle, D. Guzman-Silva, A. Perez-Leija, and A. Szameit, “Integrated photonic quantum walks,” *Journal of Optics* **18**, 103002 (2016).
- [2] M. Tillmann, B. Dakić, R. Heilmann, S. Nolte, A. Szameit, and P. Walther, “Experimental boson sampling,” *Nature Photonics* **7**, 540–544 (2013).
- [3] J. Carolan, C. Harrold, C. Sparrow, E. Martín-López, N. J. Russell, J. W. Silverstone, P. J. Shadbolt, N. Matsuda, M. Oguma, M. Itoh, G. D. Marshall, M. G. Thompson, J. C. F. Matthews, T. Hashimoto, J. L. O’Brien, and A. Laing, “Universal linear optics.” *Science (New York, N.Y.)* **349**, 711–6 (2015).
- [4] N. Spagnolo, C. Vitelli, M. Bentivegna, D. J. Brod, A. Crespi, F. Flamini, S. Giacomini, G. Milani, R. Ramponi, P. Mataloni, R. Osellame, E. F. Galvão, and F. Sciarrino, “Experimental validation of photonic boson sampling,” *Nature Photonics* **8**, 615–620 (2014).
- [5] E. Knill, R. Laflamme, and G. Milburn, “A scheme for efficient quantum computation with linear optics,” *Nature* **409**, 46–52 (2001).
- [6] U. L. Andersen, J. S. Neergaard-Nielsen, P. van Loock, and A. Furusawa, “Hybrid discrete- and continuous-variable quantum information,” *Nature Physics* **11**, 713–719 (2015).
- [7] C. Weedbrook, S. Pirandola, R. García-Patrón, N. J. Cerf, T. C. Ralph, J. H. Shapiro, and S. Lloyd, “Gaussian quantum information,” *Reviews of Modern Physics* **84**, 621–669 (2012).
- [8] X. Ma and W. Rhodes, “Multimode squeeze operators and squeezed states,” *Physical Review A* **41**, 4625–4631 (1990).
- [9] N. C. Menicucci, P. van Loock, M. Gu, C. Weedbrook, T. C. Ralph, and M. A. Nielsen, “Universal Quantum Computation with Continuous-Variable Cluster States,” *Physical Review Letters* **97**, 110501 (2006).
- [10] J. Zhang and S. L. Braunstein, “Continuous-variable Gaussian analog of cluster states,” *Physical Review A* **73**, 032318 (2006).
- [11] N. Harris, D. Bunandar, M. Pant, G. Steinbrecher, J. Mower, M. Prabhu, T. Baehr-Jones, M. Hochberg, and D. Englund, “Large-scale quantum photonic circuits in silicon,” *Nanophotonics* **5**, 456–468 (2016).
- [12] A. Dutt, S. Miller, K. Luke, J. Cardenas, A. Gaeta, P. Nussenzeig, and M. Lipson, “Tunable squeezing using coupled ring resonators on a silicon nitride chip,” *Optics Letters* **41**, 223–226 (2016).
- [13] A. Dutt, K. Luke, S. Manipatruni, A. Gaeta, P. Nussenzeig, and M. Lipson, “On-Chip Optical Squeezing,” *Physical Review Applied* **3**, 044005 (2015).
- [14] M. G. Paris, “Displacement operator by beam splitter,” *Physics Letters A* **217**, 78–80 (1996).
- [15] B. L. Schumaker, “Quantum mechanical pure states with gaussian wave functions,” (1986).
- [16] L. Wu, H. Kimble, J. Hall, and H. Wu, “Generation of Squeezed States by Parametric Down Conversion,” *Physical Review Letters* **57**, 2520 (1986).
- [17] L. Wu, M. Xiao, and H. Kimble, “Squeezed states of light from an optical parametric oscillator,” *Journal of the Optical Society of America B* **4**, 1465 (1987).
- [18] A. Lvovsky, “Squeezed Light,” in *Photonics, Volume 1: Fundamentals of Photonics and Physics, Ed. D. Andrews* (2015).
- [19] H. Vahlbruch, M. Mehmet, K. Danzmann, and R. Schnabel, “Detection of 15 dB squeezed states of light and their application for the absolute calibration of photoelectric quantum efficiency,” *Physical Review Letters* **117**, 110801 (2016).
- [20] J. W. Silverstone, D. Bonneau, K. Ohira, N. Suzuki, H. Yoshida, N. Iizuka, M. Ezaki, C. M. Natarajan, M. G. Tanner, R. H. Hadfield, V. Zwiller, G. D. Marshall, J. G. Rarity, J. L. O’Brien, and M. G. Thompson, “On-chip quantum interference between silicon photon-pair sources,” *Nature Photonics* **8**, 104–108 (2013).
- [21] M. Stefszky, R. Ricken, C. Eigner, V. Quiring, H. Herrmann, and C. Silberhorn, “Waveguide Cavity Resonator as a Source of Optical Squeezing,” *Physical Review Applied* **7**, 044026 (2017).
- [22] P. Shadbolt, M. Verde, A. Peruzzo, A. Politi, A. Laing, M. Lobino, J. Matthews, M. Thompson, and J. O’Brien, “Generating, manipulating and measuring entanglement and mixture with a reconfigurable photonic circuit,” *Nature Photonics* **6**, 45 (2012).
- [23] J. Wang, A. Santamato, P. Jiang, D. Bonneau, E. Engin, J. Silverstone, M. Lerner, J. Beetz, M. Kamp, S. Hfling,

- M. Tanner, C. Natarajan, R. Hadfield, S. Dorenbos, V. Zwiller, J. O'Brien, and M. Thompson, "Gallium arsenide (GaAs) quantum photonic waveguide circuits," *Optics Communications* **327**, 49–55 (2014).
- [24] X. Guo, C. Zou, C. Schuck, H. Jung, R. Cheng, and H. Tang, "Parametric down-conversion photon-pair source on a nanophotonic chip," *Light: Science & Applications* **6**, e16249 (2017).
- [25] N. Harris, D. Grassani, A. Simbula, M. Pant, M. Galli, T. Baehr-Jones, M. Hochberg, D. Englund, D. Bajoni, and C. Galland, "Integrated Source of Spectrally Filtered Correlated Photons for Large-Scale Quantum Photonic Systems," *Physical Review X* **4**, 041047 (2014).
- [26] M. Reck, A. Zeilinger, H. J. Bernstein, and P. Bertani, "Experimental realization of any discrete unitary operator," *Physical Review Letters* **73**, 58–61 (1994).
- [27] W. Clements, P. Humphreys, B. Metcalf, W. S. Kolthammer, and I. Walmsley, "Optimal design for universal multiphoton interferometers," *Optica* **3**, 1460–1465 (2016).
- [28] A. Yariv, "Coupled-Mode Theory for Guided-Wave Optics," *IEEE Journal of Quantum Electronics* **9**, 919 (1973).
- [29] L. Soldano and E. Pennings. "Optical multi-mode interference devices based on self-imaging: principles and applications," *Journal of Lightwave Technology* **13**, 615 (1995).
- [30] N. Spagnolo, C. Vitelli, L. Aparo, P. Matalon, F. Sciarrino, A. Crespi, R. Ramponi, and R. Osellame, "Three-photon bosonic coalescence in an integrated tritter," *Nature Communications* **4**, 1606 (2013).
- [31] P. Orlandi, F. Morichetti, M. Strain, M. Sorel, A. Melloni, and P. Bassi, "Tunable silicon photonics directional coupler driven by a transverse temperature gradient," *Optics Letters* **38**, 863 (2013).
- [32] A. Uhlmann, "The transition probability in the state space of a $*$ -algebra," *Reports on Mathematical Physics* **9**, 273 (1976).
- [33] J. P. Sprengers, A. Gaggero, D. Sahin, S. Jahanmirinejad, G. Frucci, F. Mattioli, R. Leoni, J. Beetz, M. Lerner, M. Kamp, S. Höfling, R. Sanjines, and A. Fiore, "Waveguide superconducting single-photon detectors for integrated quantum photonic circuits," *Applied Physics Letters* **99**, 181110 (2011).
- [34] B. J. Bijlani, P. Abolghasem, and Amr S. Helmy, "Semiconductor optical parametric generators in isotropic semiconductor diode lasers," *Applied Physics Letters* **103**, 091103 (2013).
- [35] F. Boitier, A. Orioux, C. Autebert, A. Lemaître, E. Galopin, C. Manquest, C. Sirtori, I. Favero, G. Leo, and S. Ducci, "Electrically Injected Photon-Pair Source at Room Temperature," *Physical Review Letters* **112**, 183901 (2014).
- [36] Z. Yan, , *in preparation*.
- [37] R. Horn, P. Kolenderski, D. Kang, P. Abolghasem, C. Scarcella, A. Frera, A. Tosi, L. Helt, S. Zhukovsky, J. Sipe, G. Weihs, A. Helmy, and T. Jennewein, "Inherent polarization entanglement generated from a monolithic semiconductor chip," *Scientific Reports* **3**, 2314 (2013).
- [38] P. Abolghasem, M. Hendrych, X. Shi, J. Torres, and A. Helmy, "Bandwidth control of paired photons generated in monolithic Bragg reflection waveguides," *Optics Letters* **34**, 2000 (2009).
- [39] S. Olivares, "Quantum optics in the phase space," *The European Physical Journal Special Topics* **203**, 3 (2012).
- [40] T. Erdogan "Optical adddrop multiplexer based on an asymmetric Bragg coupler," *Optics Communications* **157**, 249 (1998).
- [41] T. Wang, C. Chu, and C. Lin, "Electro-optically tunable microring resonators on lithium niobate," *Optics Letters* **32**, 2777 (2007).
- [42] S. Manipatruni, K. Preston, L. Chen, and M. Lipson, "Ultra-low voltage, ultra-small mode volume silicon microring modulator," *Optics Express* **18**, 18235 (2010).
- [43] D. Miller, D. Chemla, T. Damen, A. Gossard, W. Wiegmann, T. Wood, and C. Burrus, "Band-Edge Electroabsorption in Quantum Well Structures: The Quantum-Confined Stark Effect," *Physical Review Letters* **53**, 2173 (1984).
- [44] N. Menicucci, "Fault-tolerant measurement-based quantum computing with continuous-variable cluster states," *Physical Review Letters* **112**, 120504 (2014).
- [45] J. Fiurášek, "Improving entanglement concentration of Gaussian states by local displacements," *Physical Review A* **84**, 012335 (2011).
- [46] G. Xiang, T. Ralph, A. Lund, N. Walk, and G. Pryde, "Heralded noiseless linear amplification and distillation of entanglement," *Nature Photonics* **4**, 316 (2010).
- [47] A. Zavatta, J. Fiurášek, and M. Bellini, "A high-fidelity noiseless amplifier for quantum light states," *Nature Photonics* **5**, 52 (2010).
- [48] S.-H. Tan, B. I. Erkmen, V. Giovannetti, S. Guha, S. Lloyd, L. Maccone, S. Pirandola, and J. H. Shapiro, "Quantum Illumination with Gaussian States," *Physical Review Letters* **101**, 253601 (2008).
- [49] J. Niset, U. L. Andersen, and N. J. Cerf, "Experimentally Feasible Quantum Erasure-Correcting Code for Continuous Variables," *Physical Review Letters* **101**, 130503 (2008).
- [50] P. Hayden, S. Nezami, G. Salton, and B. C. Sanders, "Spacetime replication of continuous variable quantum information," *New Journal of Physics* **18**, 083043 (2016).
- [51] D. Lu, K. Li, J. Li, H. Katiyar, A. J. Park, G. Feng, T. Xin, H. Li, G. Long, A. Brodutch, J. Baugh, B. Zeng, and R. Laflamme, "Enhancing quantum control by bootstrapping a quantum processor of 12 qubits," *npj Quantum Information* **3**, 45 (2017).
- [52] B. Dive, A. Pitchford, F. Mintert, and D. Burgarth, "In situ upgrade of quantum simulators to universal computers," (2017).
- [53] S. Yokoyama, R. Ukai, S. Armstrong, C. Sornphiphatphong, T. Kaji, S. Suzuki, J. Yoshikawa, D. Yonezawa, N. Menicucci, and A. Furusawa, "Ultra-large-scale continuous-variable cluster states multiplexed in the time domain," *Nature Photonics* **7**, 982 (2013).
- [54] J. Yoshikawa, S. Yokoyama, T. Kaji, C. Sornphiphatphong, Y. Shiozawa, K. Makino, and A. Furusawa, "Generation of one-million-mode continuous-variable cluster state by unlimited time-domain multiplexing," *APL Photonics* **1**, 060801 (2016).
- [55] G. Cariolaro and G. Pierobon, "Bloch-Messiah reduction of Gaussian unitaries by Takagi factorization," *Physical Review A* **94**, 062109 (2016).
- [56] S. L. Braunstein, "Squeezing as an irreducible resource," *Physical Review A* **71**, 055801 (2005).